NASA Technical Memorandum 88909
AIAA-87-0506

The Alloy Undercooling Experiment on the Columbia STS 61-C Space Shuttle Mission

Fredric H. Harf
Lewis Research Center
Cleveland, Ohio

Thomas J. Piccone, Yanzhong Wu,
Merton C. Flemings, and Yuh Shiohara
Massachusetts Institute of Technology
Cambridge, Massachusetts

Lloyd B. Gardner
George C. Marshall Space Flight Center
Marshall Space Flight Center, Alabama

and

Edward A. Winsa
Lewis Research Center
Cleveland, Ohio

Prepared for the
25th Aerospace Sciences Meeting
sponsored by the American Institute of Aeronautics and Astronautics
Reno, Nevada, January 12-15, 1987

THE ALLOY UNDERCOOLING EXPERIMENT ON THE COLUMBIA

STS 61-C SPACE SHUTTLE MISSION

Fredric H. Harf
National Aeronautics and Space Administration
Lewis Research Center
Cleveland, Ohio 44135

Thomas J. Piccone, Yanzhong Wu, Merton C. Flemings, Yuh Shiohara
Massachusetts Institute of Technology
Cambridge, Massachusetts 02139

Lloyd B. Gardner
National Aeronautics and Space Administration
George C. Marshall Space Flight Center
Marshall Space Flight Center, Alabama 35812

Edward A. Winsa
National Aeronautics and Space Administration
Lewis Research Center
Cleveland, Ohio 44135

E-3332

SUMMARY

An Alloy Undercooling Experiment was performed in an electromagnetic levitator during the Columbia STS 61-C mission in January 1986. One eutectic nickel-tin alloy specimen was partially processed before an equipment failure terminated the experiment. Examination of the specimen showed evidence of undercooling and some unusual microstructural features.

INTRODUCTION

The Space Shuttle Columbia, launched for the STS 61-C mission on January 12, 1986, carried among its scientific payloads an electromagnetic levitator (EML). The experiment to be performed in this device required the melting in microgravity of levitated metal spheres, which would then solidify after initial undercooling. Observations of the undercooling and solidification were to be made and the resulting microstructures studied.

Solidification of a molten material requires removal of heat. This heat is composed of the specific heat of the melt and the latent heat of fusion. It is possible to remove this heat in such a manner that the material remains a liquid below its normal solidification temperature. Indeed, some materials, such as glasses, are undercooled liquids. Metals, however, normally solidify near their liquidus. Solidification is induced by nucleation promoted by inclusions or impurities, contact with containers, and vibration. In the space experiment this transformation was to be suppressed as much as possible by levitating spheres of highly purified alloys.

The instability imposed on an undercooled liquid produces a release of the heat of fusion in its transformation to the solid state. This causes the solidifying undercooled material to reheat to the vicinity of its melting temperature (fig. 1). The duration of the recalescence time, as well as the

time required for the material to solidify, decrease as the degree of undercooling increases (figs. 2 and 3) (refs. 1 and 2).

The rate of solidification plays a major role in determining the structure and properties of a material. Rapid solidification can produce a very fine grain size and suppress segregation of alloy constituents. It can even yield phases not normally obtainable in certain compositions. Undercoolings up to a few hundred Kelvins have been obtained in small levitated metal droplets on earth, in spite of vigorous convection. In space, however, larger specimens can be levitated in the absence of containers and with minimum convection. This should allow the liquid metal to undercool to a maximum extent, yield better thermal measurements and result in a greater understanding of the mechanisms of solidification.

Undercooling was to be obtained in a space experiment for three nickel-tin alloys. Details on the apparatus, launch preparations, the experiment sequence in space, and the results obtained follow.

The Alloy Undercooling program has been funded by NASA through grants and contracts NSG-7645, NAG3-597, NAS3-24383, and NAS3-24875 to the Massachusetts Institute of Technology and through contracts NAS8-33421 and NAS8-34237 to the General Electric Co. The authors recognize the contributions made to this report by G. Nathan Brown of the NASA George C. Marshall Space Flight Center and by Maria Wehrle-Due and M. Dean Dellinger of the Massachusetts Institute of Technology. Dr. George D. Nelson was Mission Specialist for the EML on the Columbia Space Shuttle orbiter. The other members of the crew were Cdr. Robert Gibson, mission commander; Lt. Col. Charles F. Bolden, pilot; Dr. Franklin Chang-Diaz, and Dr. Steven A. Hawley, mission specialists; and Robert Cenker, of RCA, and Congressman Bill Nelson, payload specialists.

EXPERIMENTAL PROCEDURES

Apparatus

The levitating and melting of specimens was carried out in an electromagnetic levitator, which is shown in figure 4, and as an inverted schematic drawing in figure 5. Technical details are given in table I.

Processing occurs in the induction cusp coil of the work chamber. When activated it carries a high frequency alternating current, which, in space at a low power level, levitates and positions the test specimen, and at a higher power level will cause heating and melting. At the end of a processing cycle levitation and positioning is maintained at a low power level, while the specimen cools and resolidifies by radiating heat to the argon atmosphere and work chamber. A mirror system is installed in the work chamber for observing the experiment by camera and pyrometry. The chamber also contains a specimen exchanger, which for this experiment had a capacity of six specimens. This exchanger loads and unloads specimens from the induction coil. Processed specimens are collected in a storage cage.

Power is provided by the Shuttle's 28-V dc supply via the MSL (Materials Science Laboratory) mounting platform. Commands originate from a panel in the aft flight deck of the crew compartment. A portion of the power is routed through the dc-to-dc converter to the housekeeping power supply which services

all control electronics, the camera, specimen changer, pyrometer, and water temperature sensor. The dc-to-dc converter provides a steady 28 volts from the incoming voltage varying between 24 and 32 V to the power amplifier, the water pump, and the pressure sensors. The power amplifier, which has three printed wiring boards that operate in parallel, converts the 28 V dc into a 100 kHz 28 V peak-to-peak signal. This power is further modified in a transformer, where impedances are matched for maximum coil efficiency. Operational controls and recycling logic are provided by sequential switching in the electronics box. A water pump circulates coolant to the induction coil, the power amplifier, and the dc-to-dc converter. Heat exchange out of the EML occurs at the base ring, where the MSL provides a cold plate with a single-phase freon cooling loop.

The EML, covered by an experiment apparatus container, is mounted on the MSL, which includes a data tape recorder, a power control box, a systems control unit, and a linear triaxial accelerometer. For the STS 61-C mission, the MSL-2 payload also included the Automated Directional Solidification Furnace and the Three-Axis Acoustic Levitator experiments as shown in figure 6 (ref. 3). The MSL-2 was located in the orbiter bay, which it shared with the Get-Away-Special (GAS)-bridge and the Hitchhiker carrier containing self-contained experiments, and a SATCOM-Ku satellite on a PAM-D2 launcher (fig. 7).

Materials

Three binary nickel-tin compositions were selected for the space experiment. Their compositions are given in table II and indicated on the phase diagram shown in figure 8. Alloys of this system had previously been used in ground-based undercooling studies (refs. 1, and 4 to 7). For the space experiment, the eutectic Ni-32.5 percent Sn alloy was to be processed first. Its liquid-solid equilibrium is at 1132 °C and when slowly cooled from the liquid its structure displays alternating face-centered cubic α phase and cubic β phase lamellae. To either side of the eutectic, at increasing liquidus temperatures, are alloys with relatively broad freezing ranges, the equilibrium microstructures for which are α phase nickel plus eutectic in the chosen "hypoeutectic" alloy and β phase plus eutectic in the "hypereutectic" alloy (table II). At 922 °C the β phase undergoes an allotropic transformation to hexagonal β' on cooling.

The specimens were prepared by melting weighed amounts of 99.99 percent purity nickel wire and 99.999 percent pure tin shot within a borosilicate glass medium, which was to act as a flux for removing impurities. The specimens were machined into spheres of approximately 8.5 mm diameter and then coated with Ferro brand EG-0222[1] silicate glass. This glass has a thermal expansion coefficient of 127×10^{-7}/K and softens at 485 °C. The purpose of the optically transparent glass coating was to protect the specimens during the long interval between specimen preparation and the flight experiment. On the hot molten specimen it was to serve as a flux which would dissolve any metal oxides so that they would not become heterogeneous nucleation catalysts and cause difficulty in achieving high undercoolings. Details on the chemical analysis, dimensions and weights for specimens carried on STS 61-C are shown in table III. Figure 9 is a photograph of a glass-coated specimen.

[1]Trademark of Ferro Corporation, Independence, OH

EML Operation

The Alloy Undercooling Experiment is performed after the Space Shuttle has obtained low earth orbit. Since the specimen is levitated in the induction coil, no special vehicle attitude is required and accelerations as great as $10^{-2} ms^{-2}$ (10^{-3} g) can be tolerated, although levels of less than $10^{-3} ms^{-2}$ (10^{-4} g) are desired (ref. 8). Thus, normal shuttle operations can be pursued, but powered orbital and attitude changes would interfere with the experiment.

The power profile of the EML coil is graphically represented in figure 10. Operations can be initiated in either the "auto" or "pause" mode. In the "auto" mode, specimens are processed consecutively without interruption. In the "pause" mode, processing for each specimen requires a separate command. Processing of a specimen consists of three successive heating/cooling cycles. In each of these cycles, spaced 3 hr apart, the specimen is to be flux-cleansed by the glass coating. In each cycle the first two minutes, with the coil at a 14 W power level, are for levitating and stabilizing the specimen. The next power level of the coil is 600 W for 2 min, during which the specimen melts and remains in the liquid state. The power then drops and stays at 14 W for 6 min, causing the levitating liquid to hopefully undercool, recalesce, solidify, and cool further. During the next three hours, the specimen is retained in the coil by the tips of thin wires located at either end of the coil, until the EML is activated for the next cycle.

The temperature of the specimen is measured by a total radiation pyrometer at a sampling rate of 125 readings per second during the 10-min levitation cycle. These data are recorded by the tape recorder of the MSL and also transmitted to ground during the orbital flight. The cooling of the specimen is observed by cinematography at 16 frames per second during 20 sec, starting 2 sec before the power reduction from 600 W.

Post Flight Analysis

After completion of the flight, the processed specimens are examined for surface and internal structures, using microprobe, and optical and electron microscopy. The structures are correlated with the temperature measurements obtained in the space experiment. Measurements of the dendrite arm spacing and other microstructural features are used to confirm the thermal data obtained by pyrometry. Comparisons are made with identical alloys which were successfully undercooled by different amounts in a normal earth-gravity environment.

PERFORMANCE OF THE SPACE EXPERIMENT

Space Flight Events

The Columbia Space Shuttle was launched on the STS 61-C mission from Kennedy Space Flight Center at 11:55'00" GMT (Greenwich Mean Time) on January 12, 1986. After orbital insertion at an altitude of about 325 km and a 28.5° inclination, the MSL was activated at 14:59' GMT. On the following day, the EML was activated at 12:23'07" GMT (T-181s), 30 sec later, the first specimen was loaded in the "pause" mode and levitated. Full power was applied at 12:26'08" GMT (T = 0).

The power transistors of the power amplifier are attached to a heat sink through which cooling water circulates. A sensor attached to this heat sink

measures its temperature, which is recorded every second and transmitted on the ground link. As shown in figure 11, this temperature was observed to rise rapidly and exceeded saturation about 120 sec after full power was applied. It was also observed that the EML power output during the 120 sec dropped from 89 to 80 percent of the planned power level, as shown in figure 12. Note that, following the heating period, the power level dropped to below that necessary for levitating the specimen. Three hours later, when the second cycle for the first specimen was to begin, the EML delivered no radio frequency (RF) power, and the unit was turned off. The EML was turned on once more on the following day, but again no RF power was generated. The specimen exchanger, however, remained functional, and the remaining specimens were unloaded into the retaining cage, in both the "pause" and "auto" mode. The EML was then deactivated.

The temperature trace as recorded is shown in figure 13. It showed intense noise contamination, especially during the 20 sec of camera operation. This trace was studied in detail and corrected, as will be explained later.

The STS 61-C mission continued as planned, and Columbia landed at Edwards Air Force Base on January 18 at 13:28' GMT.

Apparatus Failure Investigation

Following the conclusion of the 61-C mission, the EML was returned to the Marshall Space Flight Center, where it was subjected to a failure investigation. The failure investigation team performed an anomaly fault tree analysis and determined the following most probable failure scenario:

(1) The coolant loop contained gross particulate contamination. It is suspected that these particles originated during the manufacture of the EML. It appears that despite repeated cleaning they could not be removed during assembly and testing under earth gravity conditions.

(2) It is likely that the contaminant particles were dislodged by the severe vibrations during launch, and later in microgravity, carried along by the coolant. They collected in the orifice/metering area of a valve regulating the coolant flow to the power amplifier, plugging a gap of approximately 0.08 mm and reducing the flow by about 85 percent.

(3) With the coolant flow inhibited, the heat-transfer from the power transistors through the heat sink was insufficient, the power transistors overheated and failed, terminating input power to the work chamber coil.

The noise interference with the pyrometric temperature readings has also been studied. There was a constant random electrical noise causing deviations of approximately ±18 °C from the mean temperature trace during most of the heating cycle (fig. 13). This was caused by external signals intruding into an insufficiently isolated circuit. The major interference occurred during the 20 sec of camera operation. This obscured an important portion of the cooling and recalescence temperature trace. Its cause is believed to be a conducted noise generated in the speed control circuit of the Photo-Sonics 1VN motion picture camera. If confirmed by tests, it will be necessary to add special filters to eliminate this interference, or to isolate the critical circuits.

RESULTS AND DISCUSSION

Due to the early failure of the experiment apparatus, only one specimen was partially processed. This specimen as well as the temperature data have been subjected to an intensive study with the following results.

Pyrometry

The pyrometer trace summarized in figure 13 represents the propagation of heat in the metal sphere undergoing melting by high frequency induction in space. The mechanisms of heat transfer within the solid and the liquid spheres are different. When the levitated sphere is solid it essentially does not move, the surface adjacent to the coil heats up first, and the heat is conducted from there to the portion of the sphere at the open ends of coil and facing the pyrometer. Melting, which requires a substantial energy input (the heat of fusion for the eutectic is 117 kJ/kg), starts circumferentially adjacent to the coil, and from there spreads to the two poles and the center of the specimen. Once molten, electromagnetically driven flow stirs the specimen, and its temperature tends to become uniform, especially when the energy input equals the thermal losses due to radiation. When the power input terminates, the electromagnetic stirring ceases, but the specimen temperature falls essentially evenly throughout the specimen due to the high thermal conductivity of the liquid and the relatively slow rate of heat radiation to the environment. With this understanding, an interpretation of the features of the thermal history of the specimen can be made.

Details of the heating curve are shown in figure 14. Note that no arrest was observed for the β'/β transformation at 922 °C, which consumes approximately 25 kJ/kg. At about 12:26'27.7" GMT (T + 19.7s) a definite change of slope occurred when circumferential melting started adjacent to the coil. At 12:26'36" (T + 28s) there was an arrest which lasted about 4 sec (fig. 15), as the surface facing the pyrometer underwent melting. Starting about 12:26'52" (T + 44s) the energy input to the molten specimen equaled the heat losses by radiation and the temperature stabilized temporarily at about 1290 °C; but then, as the power level decreased (fig. 12), it dropped, reaching a minimum of about 1260 °C at 12:27'35" (T + 87s) (fig. 16). Note that this time corresponds to the change in slope in the heat-sink temperature (fig. 11). At this point the temperature rose slowly, reaching about 1320 °C when the camera turned on and interference obscured the trace at 12:28'05" (T + 117s). It can be speculated that either this resulted from the incipient failure of the power amplifier, or that it was caused by an accumulation of glass on the side of the specimen facing the total radiation pyrometer and by the discoloration that this glass was later observed to have acquired. Had the temperature decreased at the original rate, the temperature here would have been about 1220 °C, instead of the recorded 1320 °C, a difference of 100 °C. Proceeding now to the cooling portion of the curve (fig. 17) it can be seen that the recorded temperature is about 1230 °C at 12:28'30" (T + 142s), which is close to 100 °C above the equilibrium eutectic temperature of 1132 °C. The same figure 17 indicates that undercooling did not exceed 40 K, a disappointingly small amount, but in view of the problems encountered, logical. Traces indicating estimated actual temperatures are drawn by dashed lines in figures 14 to 17.

Specimen Surface

After the first heating cycle had been completed, the power supplied to the coil gradually decreased over 9 sec to 0 W, so that the specimen, instead of remaining levitated, drifted free and hit the retaining wire nearest the specimen exchanger. The collision occurred about 14 sec after power cut-off, as can be judged from timing the film sequence which covered the 20 sec about the power cut-off. At this time, the specimen was still molten. The film, which is not well focused, does not, however, make clear why the glass collected around the wire. It is possible that, for some reason, the glass had drifted to one side of the specimen even while the coil was under full power, and this assumption is certainly in line with inconsistencies in the temperature-time trace. At any rate, eventually at least a partial separation occurred between the wire and the specimen, providing a one ohm resistance between the two parts.

When the specimen exchanger was activated later during the flight, it pushed the specimen through the coil into the cage, and may have broken the high carbon steel retaining wire, which had been severely annealed when it plunged into the molten glass. The specimen, as recovered, is shown in figure 18. Note that on the side opposite the wire it is bare and no longer glass-covered. Apparently some of the glass had flowed along the wire for some distance, because the processed specimen plus the attached wire weighed 0.0258 g less than the glass-coated specimen alone before loading into the EML. The previously colorless transparent glass had turned brown, and its surface was very smooth and highly reflective.

Low magnification photographs of the exposed metal surface and the metal surface below the removed glass layer are shown in figure 19. A hole in the surface was found below the glass layer near the embedded end of the wire. Upon cross-sectioning the specimen, this hole was found to be a large solidification shrinkage cavity, as shown in figure 20. The metal surface not covered by glass displayed several shallow dimples caused by solidification shrinkage, and was partly rough and partly smooth in appearance.

The smooth part of the surface contained the apparently sole nucleation site, which is shown in figure 21. The longest surface dendrite proceeds from this site. Several large dendrites were found on the smooth surface region. The dendrites are well-developed, with apparent primary, secondary, and tertiary arms (fig. 22). Dendritic structures have sometimes been observed on surfaces of eutectic samples used in ground-based work when there was moderate (more than 100 K) undercooling (ref. 9). Dendrites would not be expected, and have not been observed, in samples solidified with very low undercooling.

Because the specimen is of eutectic composition, the presence of large dendrites on its surface is remarkable. Normally, a Ni-Sn eutectic sample without undercooling solidifies with a lamellar two-phase structure, such as the structure shown in figure 23. An important aspect of these "dendrites" of the flight specimen is that their main branches are curved. The radius of curvature of the dendrite shown in figure 21 is about 2 mm. Such severely curved dendrites have not been observed in ground-based work with Ni-Sn alloys. It is believed that the curving of dendrites is due to thermal stresses within the dendrite resulting from steep thermal gradients during recalescence, or mechanical stresses resulting from solidification shrinkage and convection during dendrite growth. The curvature of the dendrites is determined by heat

flow and/or fluid flow, not by the preferred lowest energy orientation (ref. 10).

Another significant aspect of these dendrites is that, for the most part, the secondary arms do not appear to be perpendicular to the primary arms, and the tertiary arms are likewise not orthogonal to the secondary arms. This can be seen in the photographs of dendrite arms in figure 22. The angle between the apparent primary and secondary arms varies between about 45° and 75°. Some of the variation may be due to the curvature of the surface as a function of position. When dendrites have been observed in ground-based work on relatively highly undercooled Ni-Ni_3Sn eutectic alloy samples, the secondary arms were perpendicular to the primary arms.

Because the specimen did not attain a large undercooling before nucleation, it would be expected that the structure would mainly be composed of normal lamellar eutectic. A photograph of a region of normal eutectic structure, from the metal surface under the glass layer, is shown in figure 23, together with that of the surface structure of a ground-based eutectic sample with 31 K initial undercooling. The structures are similar.

A number of small patches of anomalous eutectic microstructure were found on the surface of the specimen (fig. 24). Their structure is composed of the same two phases as the lamellar structure; this morphology is only observed when there is at least some initial undercooling. The presence of anomalous eutectic is proof that some undercooling was attained, although the amount of undercooling may still be less than 40 K, as discussed later.

Another feature discovered was a fine structure having the appearance of two-phase "particulates." This structure is shown in figure 25. The dark spots in the small depressions, which are of submicron size, appear to be solid state precipitates. These probably formed during cooling in the solid state due to the decreasing solubility of tin in the nickel-rich α phase with decreasing temperature. Such precipitates have also been observed in polished and etched cross-sections of ground-based samples.

Several fragments of dendrites with extremely fine secondary arm spacing were found on the surface of the flight specimen. One example is shown in figure 26. The retention of such a fine arm spacing indicates that the dendrite was isolated from the remaining liquid by decanting due to shrinkage during solidification, and therefore did not coarsen appreciably.

The surface of the shrinkage cavity also showed lamellar and anomalous eutectic structures, as shown in figure 27. Figure 28 shows a region of anomalous eutectic structure from the surface of a ground-based eutectic sample with 31 K initial undercooling. This is very similar to the structure in the shrinkage cavity of the flight specimen.

The bottom of the shrinkage cavity, shown in figure 29(a), contained a multitude of small faceted crystals, of which two are shown in detail in figure 29(b). Their origin will be discussed in the next section.

Cross-Sectional Microstructures

The cross-sectional microstructure of the flight specimen consisted mainly of normal lamellar eutectic. A typical structure is shown in figure 30.

Figure 31 is a very similar structure from a ground-based eutectic sample with 31 K initial undercooling. The volume fraction of lamellar eutectic in the cross-sectional microstructure of the flight specimen was measured at over 90 percent, which corresponds to an initial undercooling of less than 30 K (ref. 11).

Faceted crystals were also found in the cross-sectional microstructure. They were dispersed throughout the bulk of the specimen, as seen in the low magnification photograph in figure 32(a). When observed at higher magnification, it appears that the eutectic may have nucleated on some of the crystals, as shown in figure 32(b). Energy-dispersive X-ray analysis revealed that these crystals contain a measurable amount of iron, and little tin, while the surrounding matrix contains no detectable iron. This finding indicates that part of the steel retaining wire found embedded in the glass had penetrated and dissolved in the metal sample while it was molten, and may have indirectly caused nucleation of the specimen, thereby causing low undercooling.

Other Data and Results

The specimen mass before processing was 3.0695 g, consisting of 2.9983 g of metal and 0.0712 g of glass. After processing, the specimen mass was 3.0437 g, including a short piece of steel wire weighing 0.0015 g. The mass loss of the processed specimen (metal and glass) is 0.0273 g.

The piece of steel wire was separated from the glass and examined by optical and scanning electron microscopy. The wire has a bend of more than 60° near its center. Its end-to-end length is 3.05 mm, and its diameter is 0.25 mm. The compositions at the two ends of the wire were qualitatively measured using energy-dispersive X-ray analysis. One end was covered with a small cap of metal, which was found to be almost entirely composed of nickel and tin. This is a definitive proof that the wire had contacted the molten alloy sample during processing. The other end, which is presumed to be a fracture surface, showed only iron at one location, and at another location showed some silicon and sodium (from the glass), as well as some nickel and tin. From the appearance of the surface at this end of the wire, it is difficult to determine whether there was contact with the glass and metal from the specimen, or simply contamination due to the process of removal of the glass from the specimen surface.

Fragments of the glass were examined by transmitted light microscopy. This revealed that the coloration of the glass is nonuniform. Portions of the glass are transparent, and other portions are very dark in color. The coloration is apparently due to impurities introduced into the glass by chemical reactions, but this has not yet been substantiated.

CONCLUDING REMARKS

Although this experiment was cut short, the capability of the electromagnetic levitator to process specimens in the Space Shuttle environment was demonstrated. The apparatus levitated the specimen, caused it to melt, and kept it at temperature for a predetermined length of time. In the single completed heating cycle, the thermal history and microstructure indicate that the undercooling reached about 30 K. The microstructure contained some unique features, but most of the results are very similar to those of a ground-based sample with 31 K initial undercooling. Had the planned triple cycling been

completed this undercooling very likely would have increased and produced a more unique microstructure, especially in the off-eutectic compositions.

REFERENCES

1. Piccone, T.J., Wu, Y., Shiohara, Y., and Flemings, M.C., "Dendritic Growth of Undercooled Nickel-Tin: Part II," Metallurgical Transactions A, in press.

2. Piccone, T.J., "Thermal History and Microstructure of Undercooled Nickel-Tin Alloys," S. M. Thesis, Massachusetts Institute of Technology, 1984.

3. "MSL-2," NASA Marshall Space Flight Center, 1985. (Government Printing Office 1985-631-058/20046)

4. Flemings, M.C. and Shiohara, Y., "Solidification of Undercooled Metals," Materials Science and Engineering, Vol. 65, 1984, pp. 157-170.

5. Wu, Y., Piccone, T.J., Shiohara, Y., and Flemings, M.C., "Structure and Recalescence Behavior of Undercooled Nickel-Tin Alloys," Rapidly Solidified Metastable Materials, B.H. Kear and B.C. Giessen, eds., Elsevier, New York, 1984, pp. 37-42

6. Yamamoto, M., Wu, Y., Shiohara, Y., and Flemings, M.C., "Comparison of Structures of Gas Atomized and of Emilsified Highly Undercooled Ni-Sn Alloy Droplets," Rapidly Solidified Alloys and Their Mechanical and Magnetic Properties, B.C. Giessen, D.E. Polk, and A.I. Taub, eds., Materials Research Society, Pittsburgh, PA, 1986, pp. 411-414.

7. Shiohara, Y., Flemings, M.C., Wu, Y., and Piccone, T.J., "Rapid Solidification of Levitation Melted Ni-Sn Alloy Droplets with High Initial Undercooling," Tetsu-to-Hagane, No. 10, Vol. 71, 1985, A209-212.

8. "MSL-2 Instrument Interface Agreement for Electromagnetic Levitator (EML)," JA-367, NASA Marshall Space Flight Center, Sept. 1983.

9. Wu, Y., "Solidification of Undercooled Nickel-Tin Alloys," Sc.D. Thesis, Massachusetts Institute of Technology, 1986.

10. Bower, T.F., and Flemings, M.C., "Structure of Dendrites at Chill Surfaces," Transactions of the AIME, Vol. 239, Oct. 1967, pp. 1620-1625.

11. Wu, Y., Piccone, T.J., Shiohara, Y., and Flemings, M.C., "Dendritic Growth of Undercooled Nickel-Tin: Part III," to be published in Metallurgical Transactions A, 1987.

TABLE I. - SELECTED DATA FOR ELECTROMAGNETIC LEVITATOR

Manufacturer: General Electric Company, Space Division, Valley Forge, PA.

Weight: EML 47.7 kg, cover 27.8 kg

Height: 61 cm, without base or cover

Diameter: 35 cm at frame

Power Input: 28 V dc through 80 amp fused circuit

Induction Heating: 600 W at 100 kHz

Coil: 3.2 mm OD, 1.6 mm ID copper tubing, with water flow at 8 $cm^3 s^{-1}$

Work chamber coolant flow: 14 $cm^3 s^{-1}$ through 4.8 mm ID tubing

dc-to-dc converter, 50 percent efficiency factor

Camera: Photo-Sonics, Model 1VN, with magazine for 60 m of 16 mm film

Pyrometer: Total radiation

TABLE II. - PROPERTIES OF TEST ALLOYS

Designation	Tin content, wt % (nickel base)	Liquidus, °C	Solidus, °C	Aver. specific heat, J kg^{-1} K^{-1}	Latent heat of fusion, kJ kg^{-1}
Eutectic	32.5	1132	1132	500	117
Hypoeutectic	25	1224	1132	500	150
Hypereutectic	37.5	1169	1132	500	90

Latent heat of β/β' transformation 25 kJ kg^{-1}

TABLE III. - SPECIMENS CARRIED IN EML DURING STS 61-C MISSION

Number[a]	Analyzed tin content, wt %	Bare metal sphere		Glass-coated sphere	
		diameter[b] mm	weight g	diameter[b] mm	weight g
1	32.50	8.48	2.998	8.73	3.070
2	32.52	8.45	2.982	8.78	3.064
3	37.49	8.45	2.917	8.65	2.975
4	37.47	8.48	3.000	8.68	3.053
5	24.96	8.72	3.142	8.97	3.216
6	24.96	8.72	3.006	8.96	3.088

[a]Sequence in which specimens were to be processed
[b]Average measurements

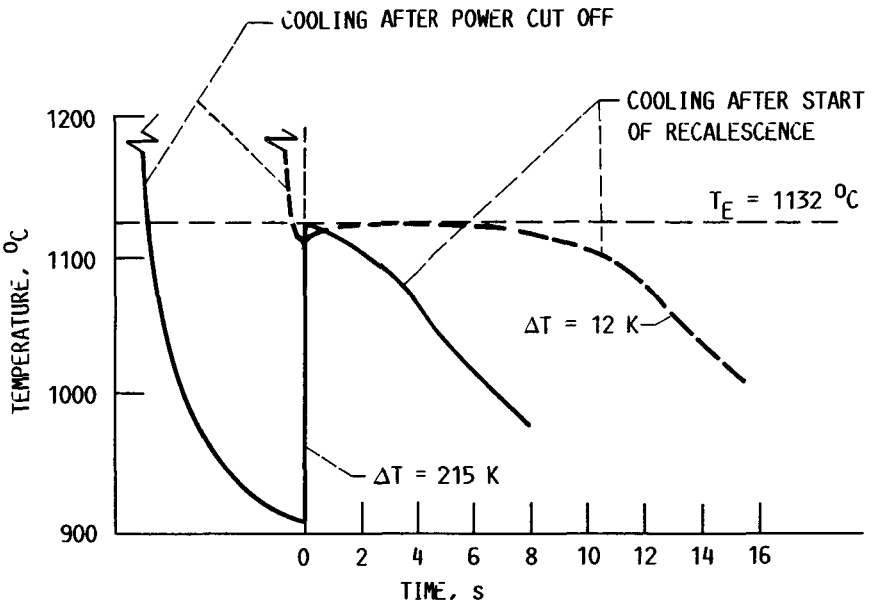

FIGURE 1.- COOLING CURVES FOR EUTECTIC NICKEL-TIN ALLOY AT TWO LEVELS OF UNDERCOOLING.

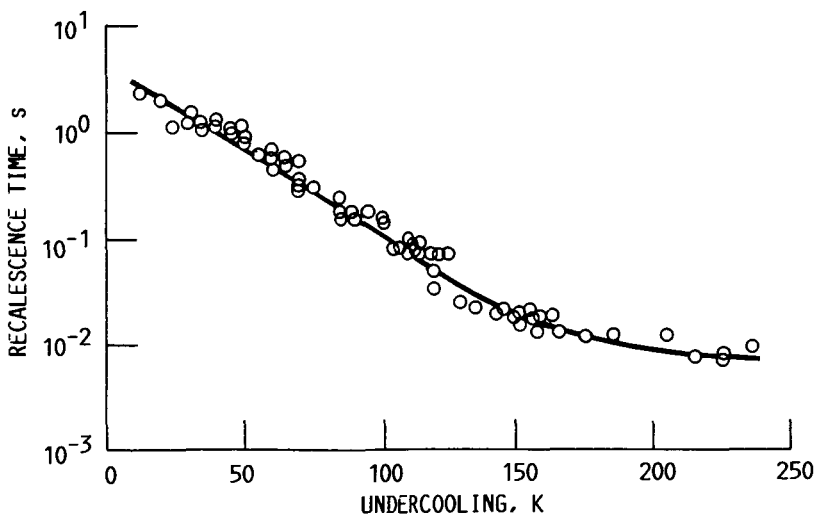

FIGURE 2. - RECALESCENCE TIME AND INITIAL UNDERCOOLING FOR 3.2 GRAM NICKEL-TIN EUTECTIC SAMPLES (REF. 2).

ORIGINAL PAGE IS
OF POOR QUALITY

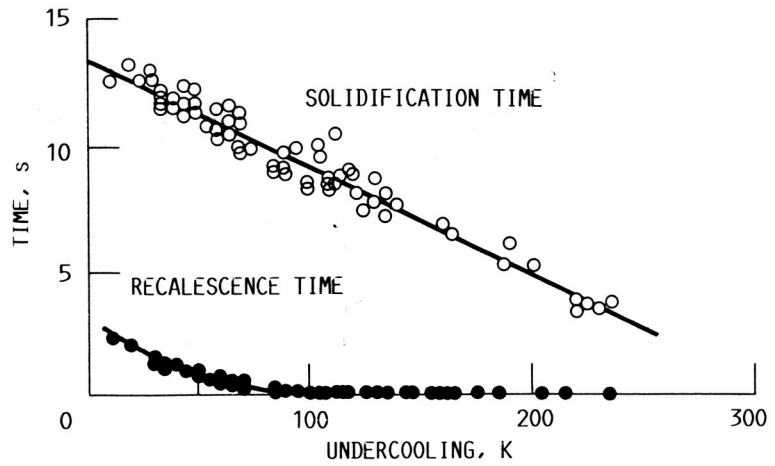

FIGURE 3. - EFFECT OF INITIAL UNDERCOOLING ON SOLIDIFICATION AND RECALESCENCE TIME IN 3.2 GRAM NICKEL-TIN EUTECTIC SAMPLES (REF. 1).

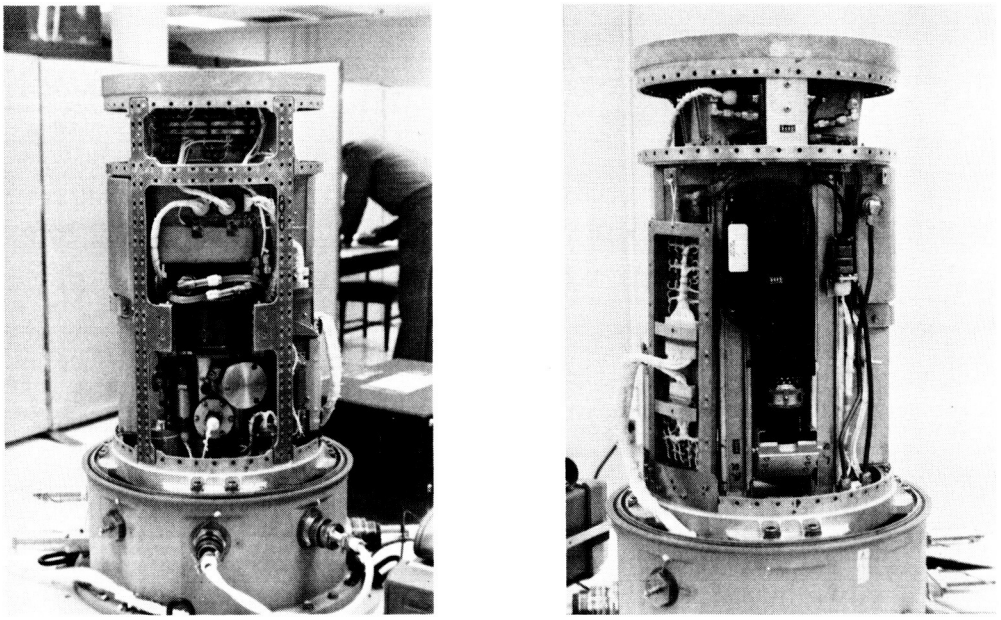

(A) WORKCHAMBER SIDE (B) CAMERA SIDE

FIGURE 4. - ELECTROMAGNETIC LEVITATOR SEEN FROM THE WORKCHAMBER SIDE AND THE CAMERA SIDE.

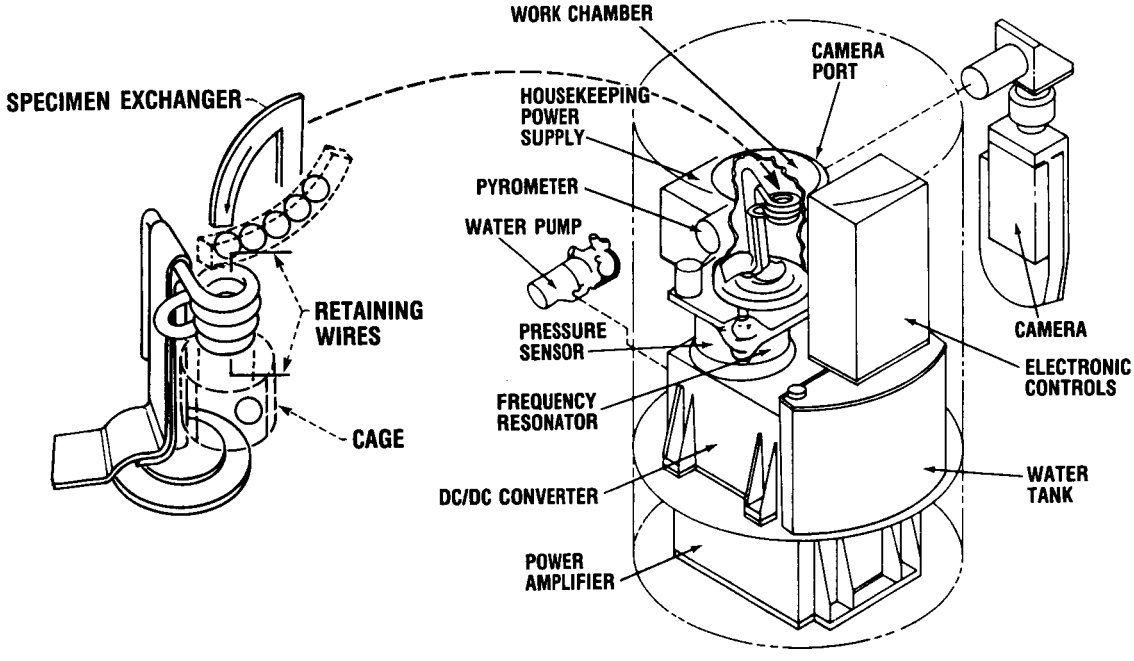

FIGURE 5. - WORKING COMPONENTS OF ELECTROMAGNETIC LEVITATOR USED IN ALLOY UNDERCOOLING EXPERIMENT.

CD-86-23813

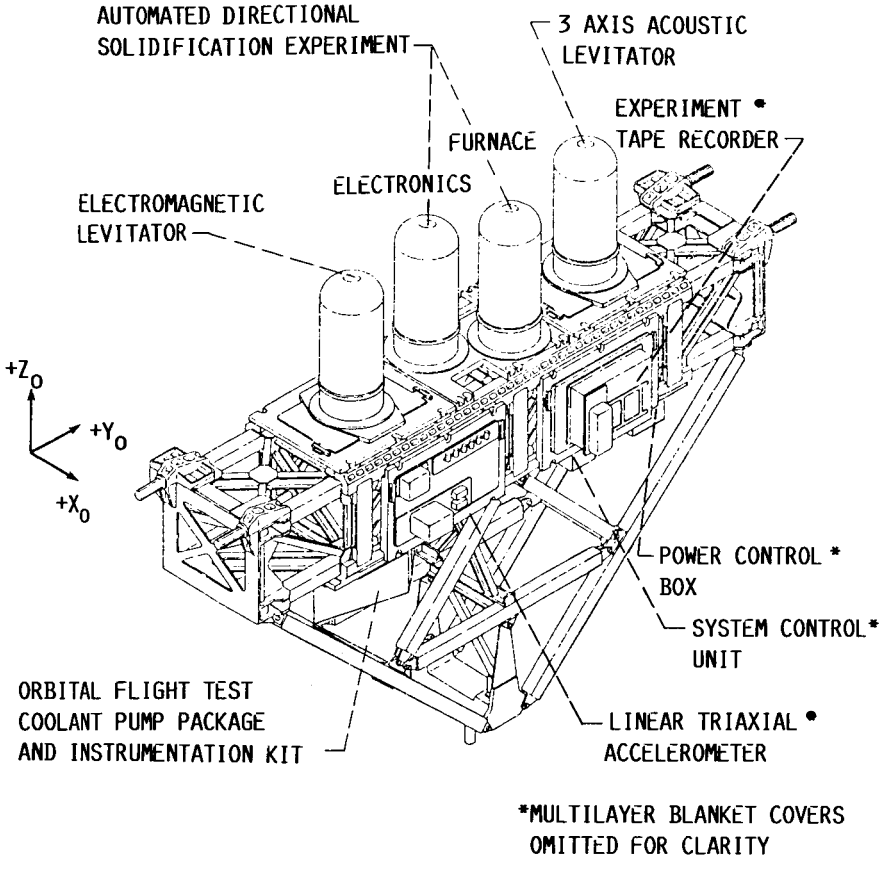

FIGURE 6. - MSL-2 CONFIGURATION FOR STS 61-C SPACE MISSION.

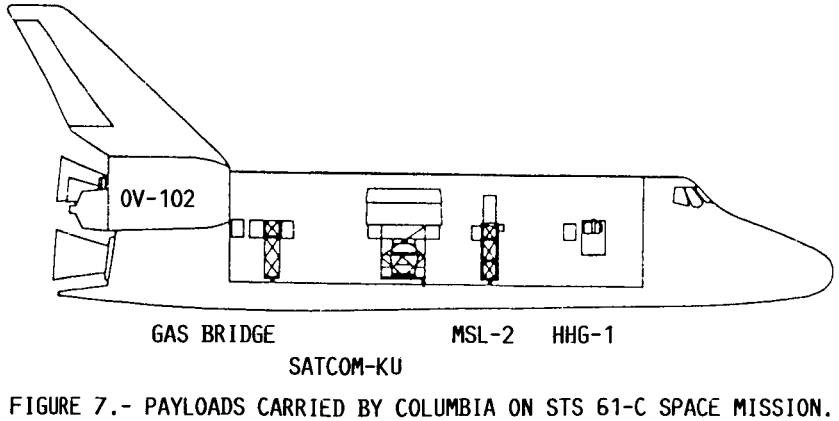

FIGURE 7.- PAYLOADS CARRIED BY COLUMBIA ON STS 61-C SPACE MISSION.

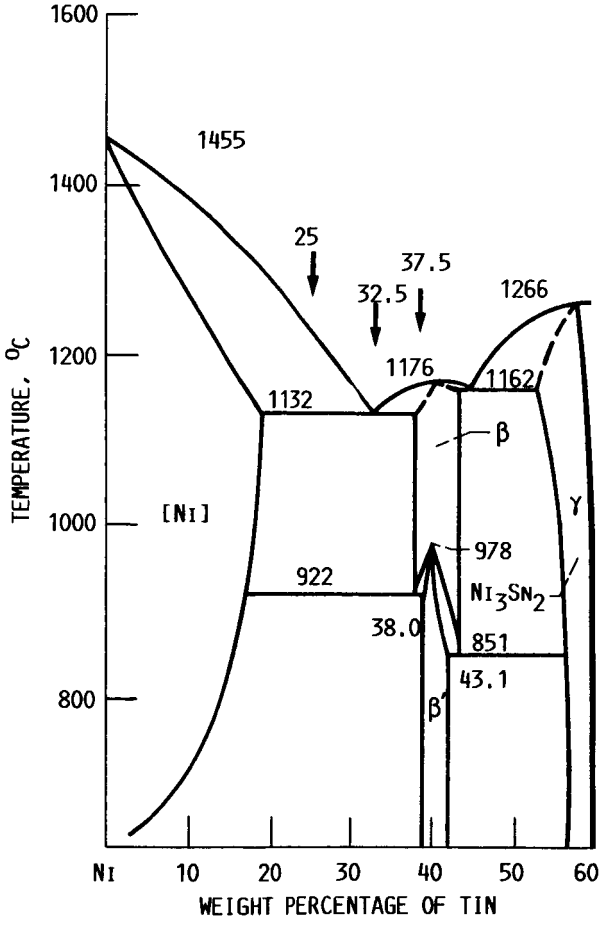

FIGURE 8.- THE NICKEL-RICH PART OF THE NICKEL-TIN PHASE DIAGRAM. ARROWS AT 25, 32.5 AND 37.5 WEIGHT PERCENT TIN INDICATE HYPOEUTECTIC, EUTECTIC AND HYPEREUTECTIC COMPOSITIONS.

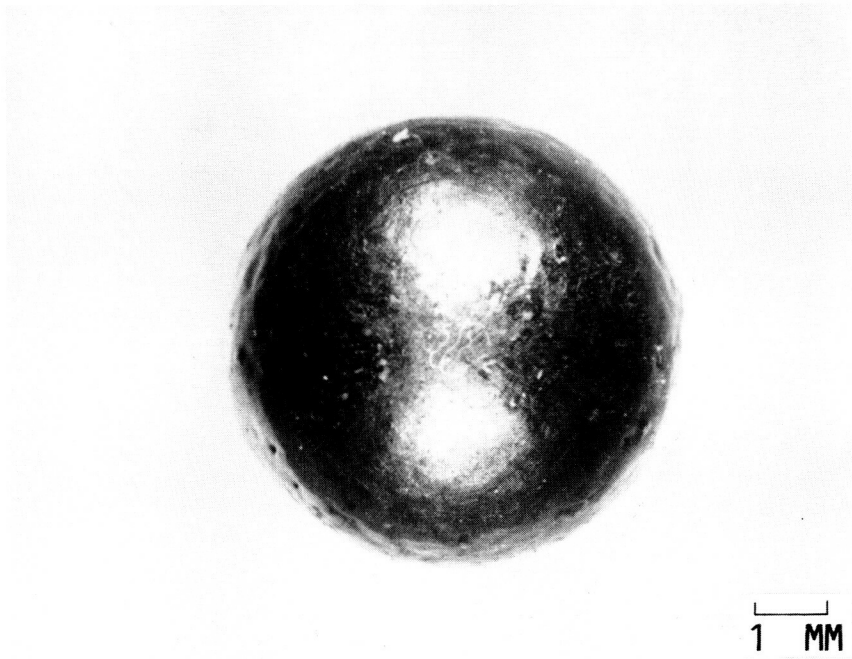

FIGURE 9. - GLASS-COATED NICKEL-TIN ALLOY SPECIMEN PREPARED FOR PROCESSED IN ELECTROMAGNETIC LEVITATOR ON STS 61-C MISSION.

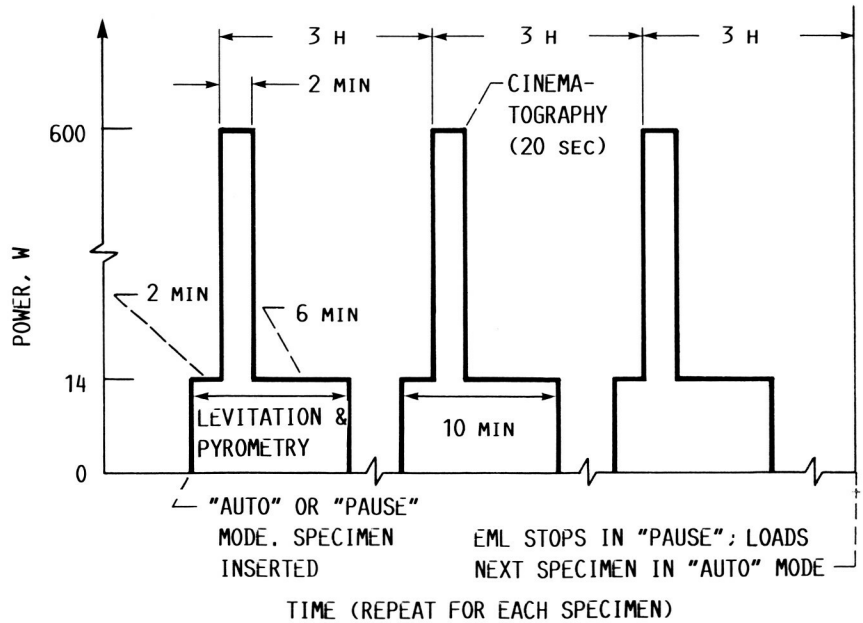

FIGURE 10.- INDUCTION COIL POWER PROFILE FOR ONE SPECIMEN IN THE ELECTROMAGNETIC LEVITATOR.

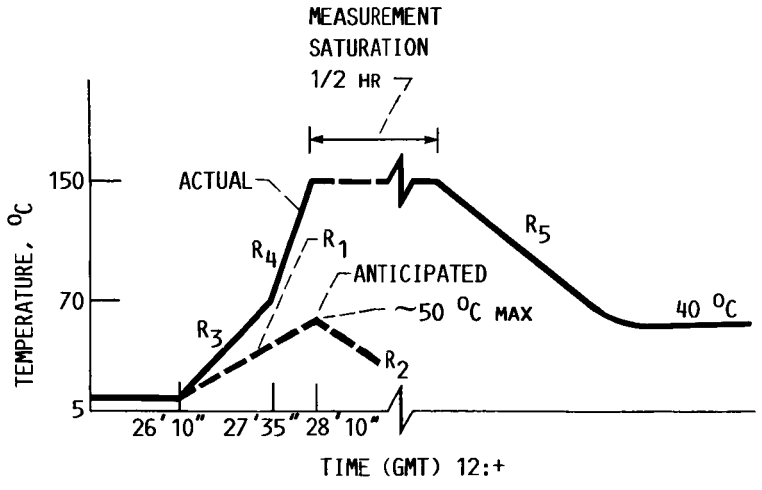

FIGURE 11.- ANTICIPATED AND ACTUAL TEMPERATURES IN HEAT SINK OF POWER AMPLIFIER DURING FIRST HEATING CYCLE OF ELECTROMAGNETIC LEVITATOR. RATES OF TEMPERATURE CHANGE: ARE R_1 = 0.36 Ks^{-1}, R_2 =- 0.22 Ks^{-1}, R_3 = 0.75 Ks^{-1}, R_4 = 1.3 Ks^{-1}, R_5 ≅- 0.05 Ks^{-1}.

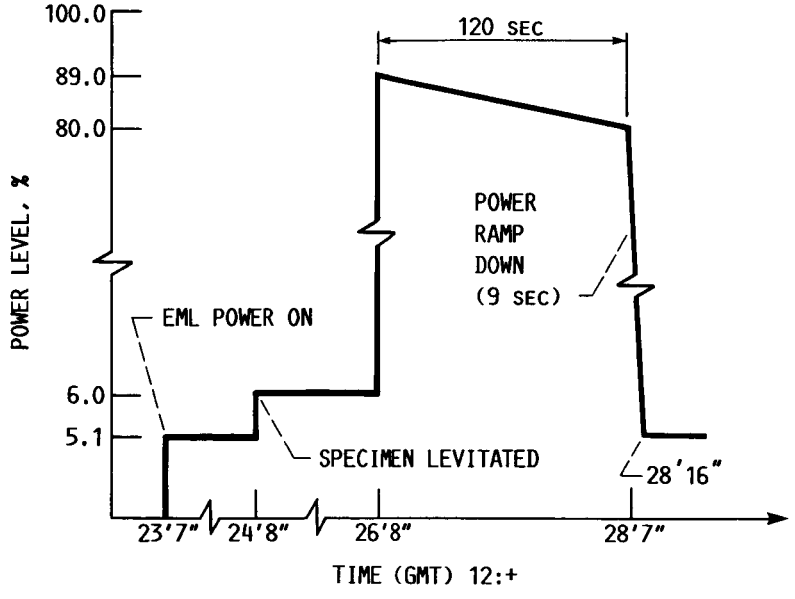

FIGURE 12. - POWER LEVEL MEASURED AT ELECTROMAGNETIC LEVITATOR CONTROL STATION SHOWING A 9% POWER LEVEL VARIANCE DURING THE FIRST HEATING CYCLE.

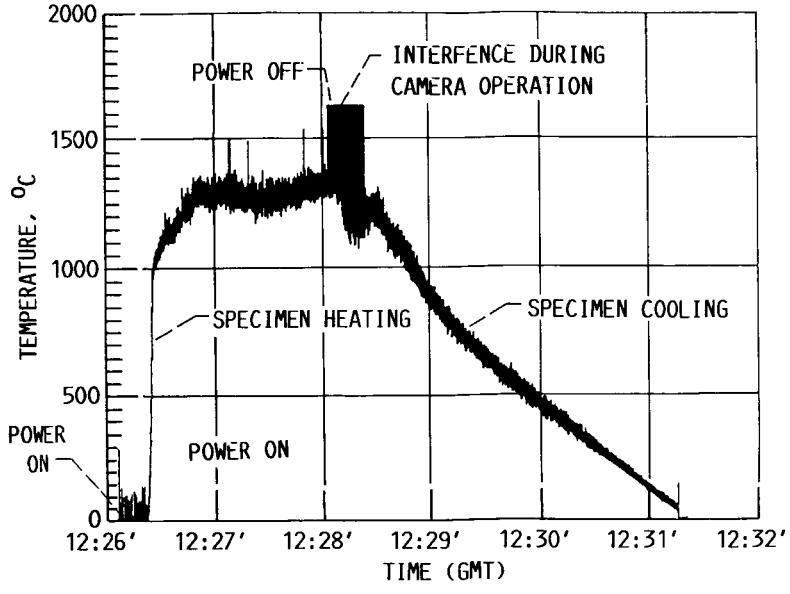

FIGURE 13. - TEMPERATURE OF EUTECTIC NICKEL-TIN ALLOY SPECIMEN DURING HEATING CYCLE, MEASURED BY PYROMETER, RECORDED AT 125 s^{-1}.

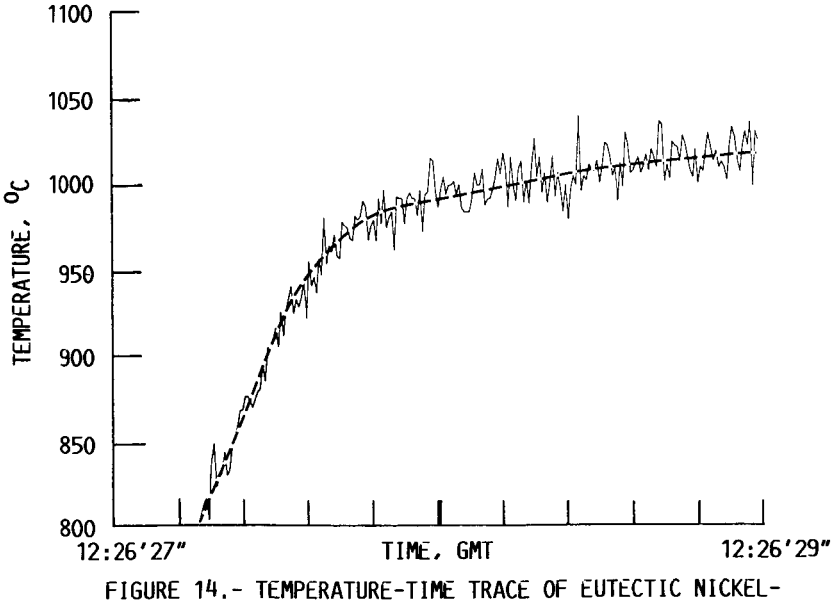

FIGURE 14.- TEMPERATURE-TIME TRACE OF EUTECTIC NICKEL-TIN ALLOY SPECIMEN DURING 2 sec OF HEATING, 125 PYROMETER READINGS PER sec. DASHED LINE SHOWS ESTIMATED ACTUAL TEMPERATURE.

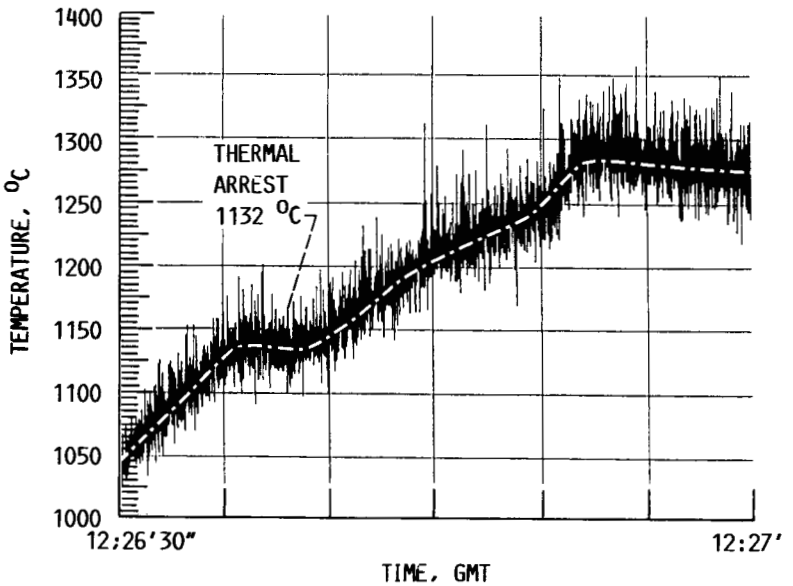

FIGURE 15.- TEMPERATURE-TIME TRACE OF EUTECTIC NICKEL-TIN ALLOY DURING 30 SEC OF HEATING SHOWING EUTECTIC MELTING THERMAL ARREST ABOUT 12:26'38" GMT, 125 PYROMETER READINS PER SEC. BAND WIDTH CAUSED BY EXTERNAL INTERFERENCE. DASHED LINE SHOWS ESTIMATED ACTUAL TEMPERATURE.

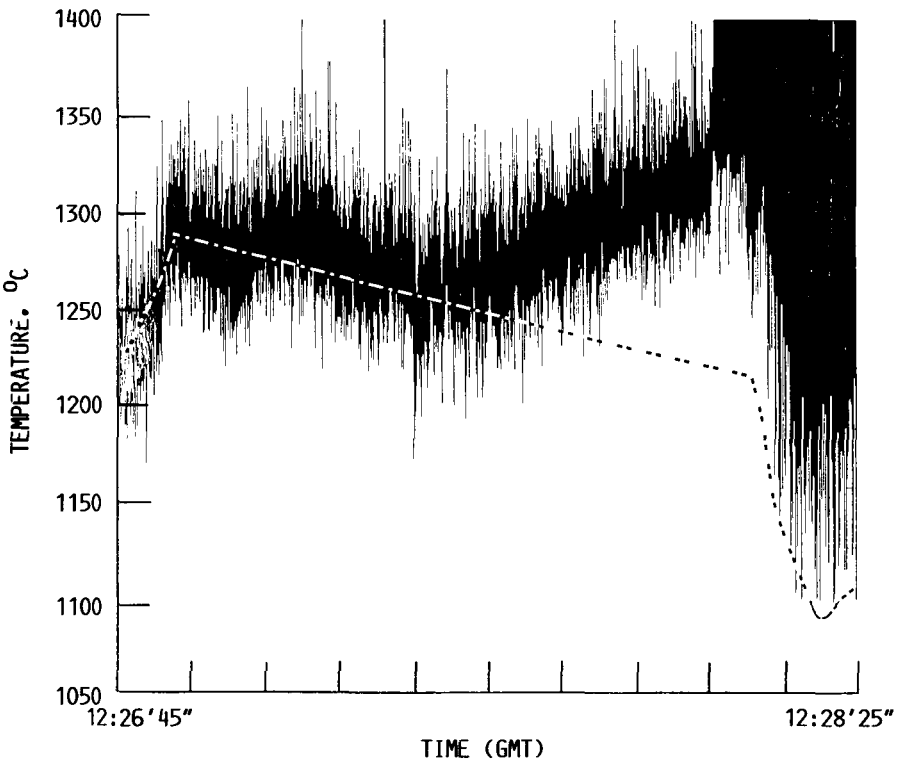

FIGURE 16. - TEMPERATURE-TIME TRACE OF EUTECTIC NICKEL-TIN ALLOY DURING 100 SECONDS IN MOLTEN STATE, 125 PYROMETER READINGS PER SECOND. BAND WIDTH CAUSED BY EXTERNAL INTERFERENCE AND STARTING 12:28'5" BY CAMERA. DASHED LINES SHOWS ESTIMATED ACTUAL TEMPERATURE.

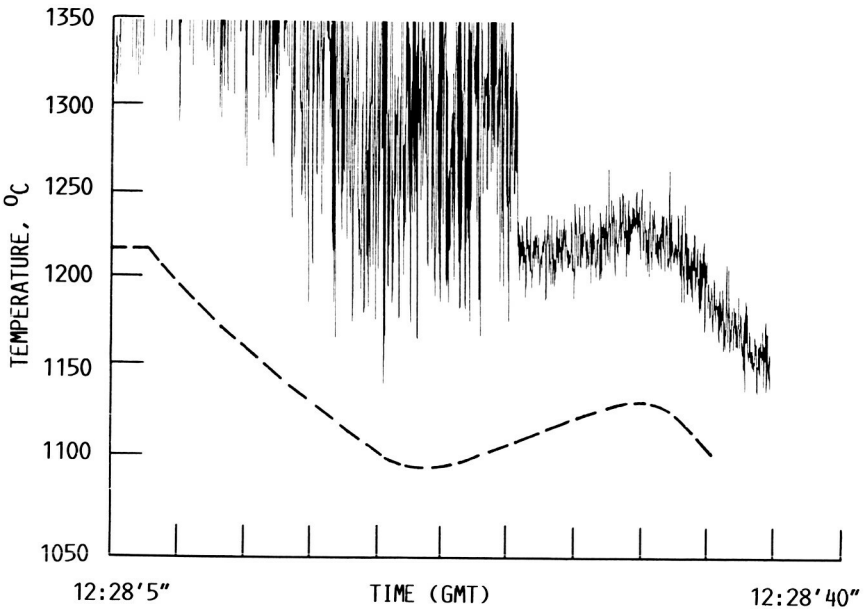

FIGURE 17.- TEMPERATURE-TIME TRACE OF NICKEL-TIN ALLOY DURING 40 SECONDS OF COOLING, 125 PYROMETER READINGS PER SECOND. BAND WIDTH, CAUSED BY CAMERA UNTIL 12:28'26", REMAINDER BY OTHER INTERFERENCE, PARTLY REMOVED BY BAND PASS FILTERING. DASHED LINE SHOWS ESTIMATED ACTUAL TEMPERATURE.

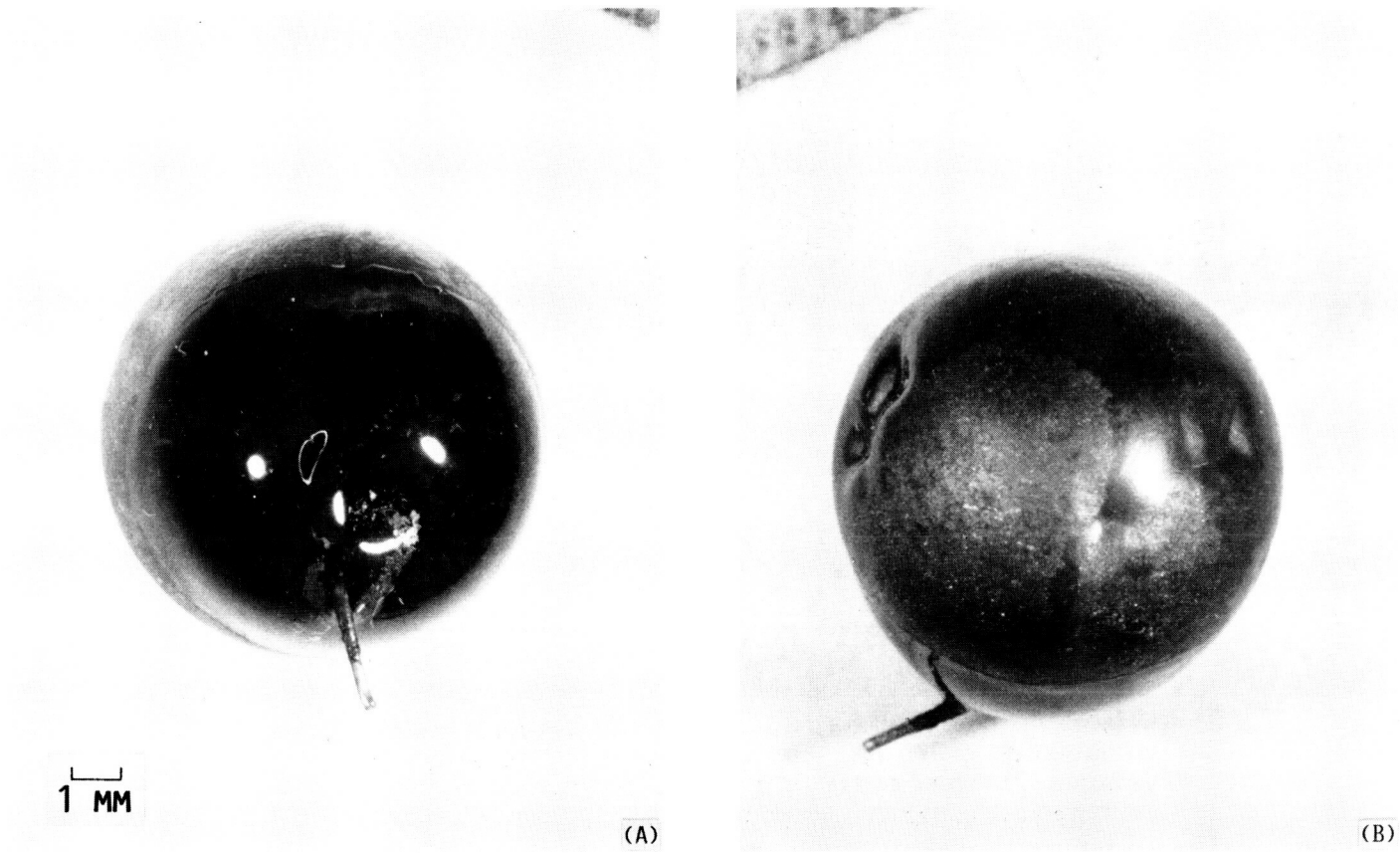

FIGURE 18. - TWO VIEWS OF THE NICKEL-TIN EUTECTIC ALLOY SPECIMEN PROCESSED IN THE ELCTROMAGNETIC LEVITATOR. A PORTION OF THE RETAINING WIRE CAN BE SEEN EMBEDDED IN THE GLASS, WHICH HAS AGGLOMERATED TO ONE SIDE OF THE SPECIMEN.

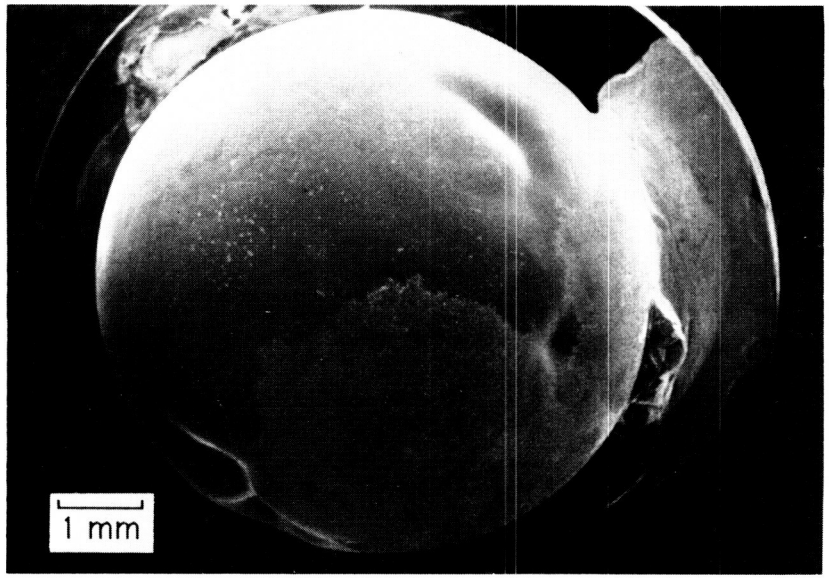

(A) EXPOSED METAL SURFACE.

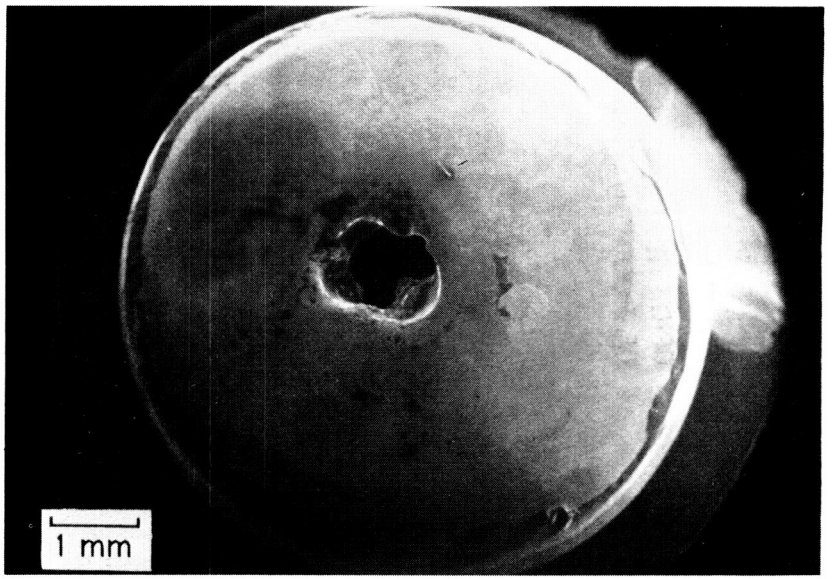

(B) METAL SURFACE WITH CAVITY BELOW THE REMOVED GLASS LAYER.

FIGURE 19. - SCANNING ELECTRON MICROGRAPHS OF THE FLIGHT SPECIMEN AFTER PROCESSING.

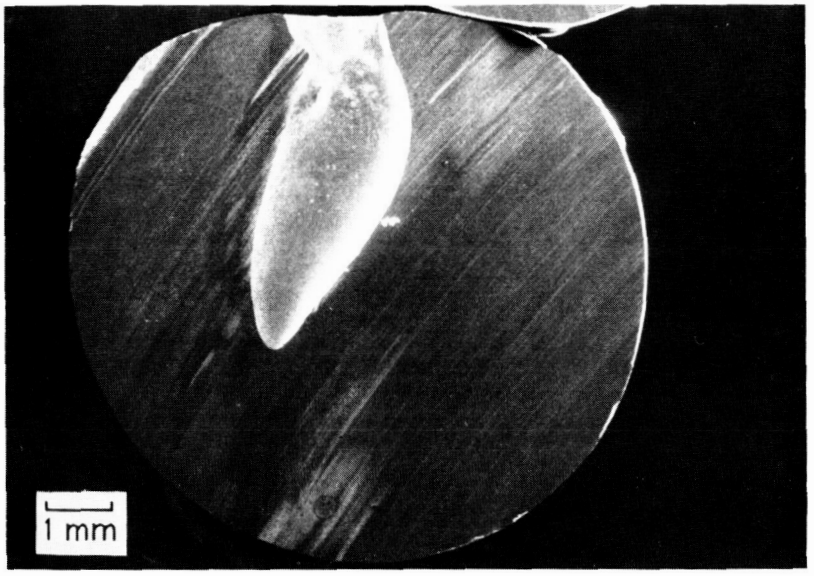

FIGURE 20. - CROSS-SECTION OF FLIGHT SPECIMEN, SHOWING THE LARGE SHRINKAGE CAVITY.

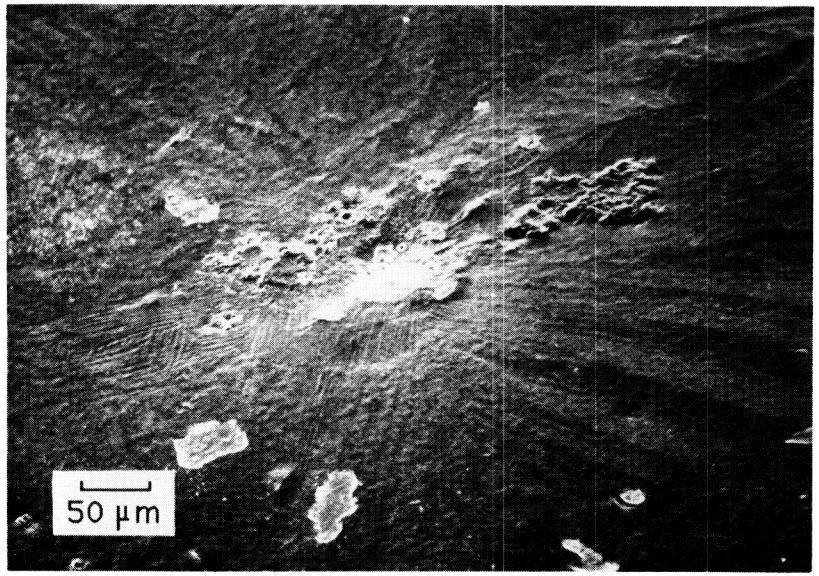

(A) AT HIGH MAGNIFICATION.

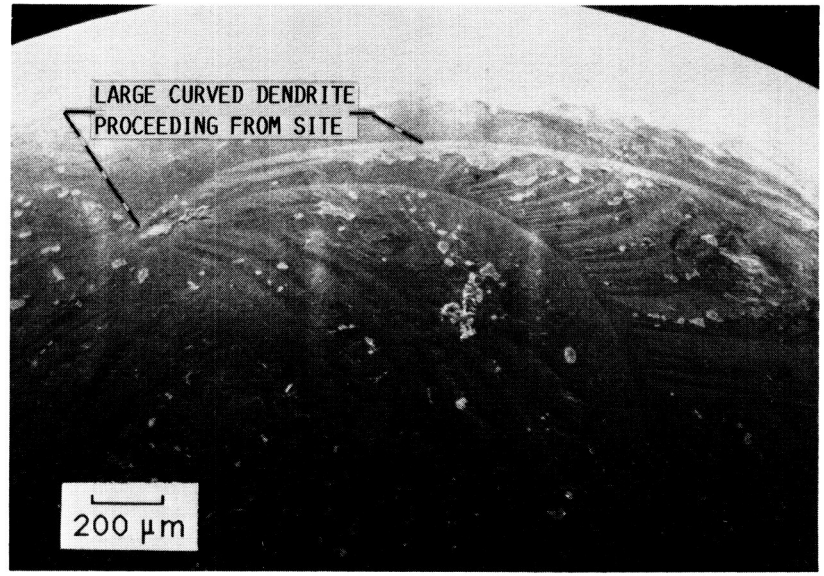

(B) AT LOWER MAGNIFICATION.

FIGURE 21. - APPARENT NUCLEATION SITE ON SURFACE OF PROCESSED NICKEL-TIN EUTECTIC FLIGHT SPECIMEN.

FIGURE 22. - TWO VIEWS OF DENDRITES ON SURFACE OF NICKEL-TIN EUTECTIC ALLOY FLIGHT SPECIMEN.

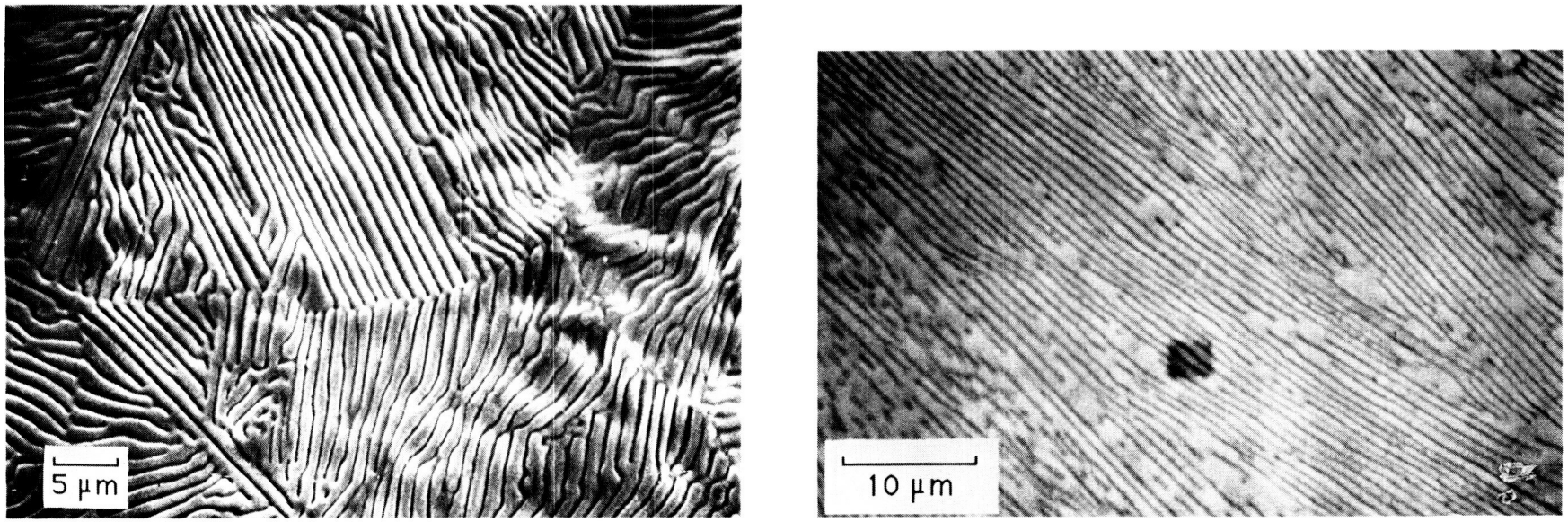

(A) FLIGHT SPECIMEN.

(B) 3.2 GRAM GROUND-BASED EUTECTIC SAMPLE WITH 31 K INITIAL UNDERCOOLING.

FIGURE 23. - NORMAL LAMELLAR EUTECTIC STRUCTURES ON THE SURFACE.

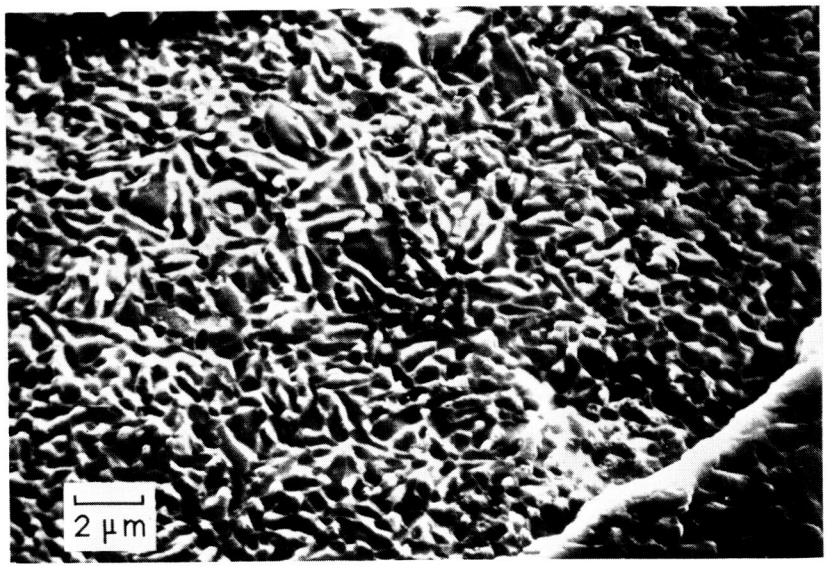

FIGURE 24. - PATCH OF ANOMALOUS EUTECTIC STRUCTURE ON THE FLIGHT SPECIMEN SURFACE.

FIGURE 25. - FINE TWO-PHASE STRUCTURE ON THE FLIGHT SPECIMEN SURFACE.

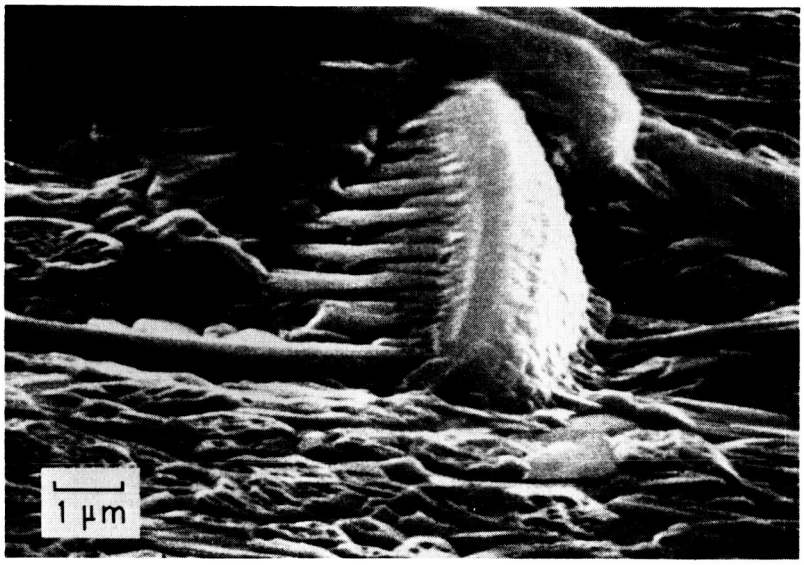

FIGURE 26. - DENDRITE FRAGMENT ON THE FLIGHT SPECIMEN SURFACE.

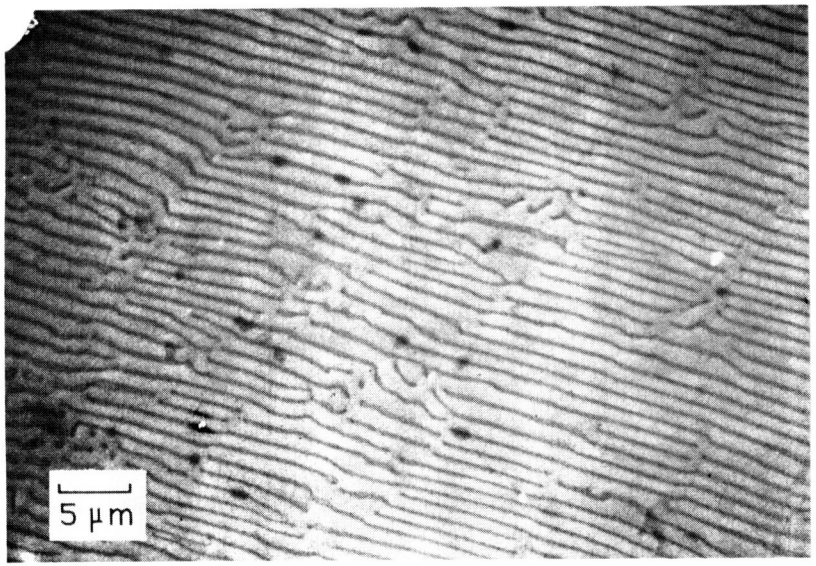

(A) LAMELLAR.

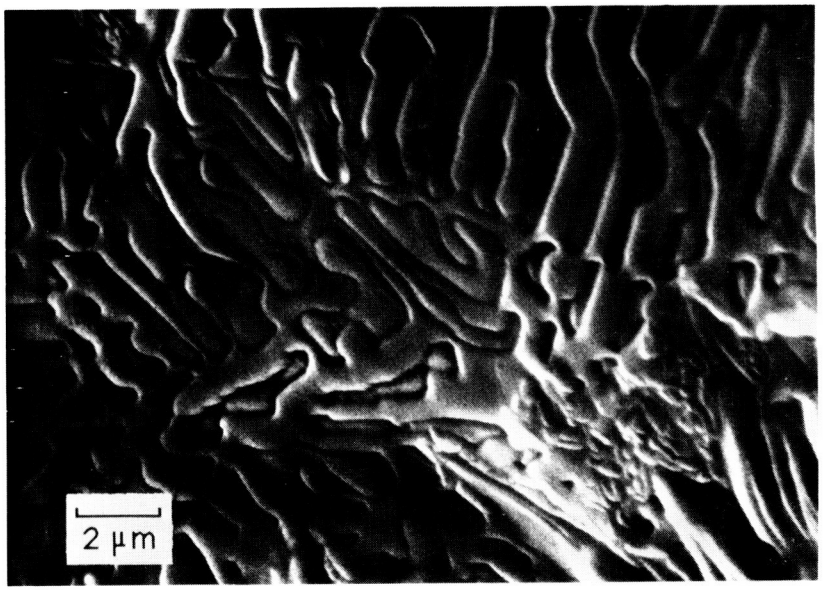

(B) ANOMALOUS.

FIGURE 2. MICROSTRUCTURES ON THE SURFACE OF THE SHRINKAGE CAVITY IN THE FLIGHT SPECIMEN.

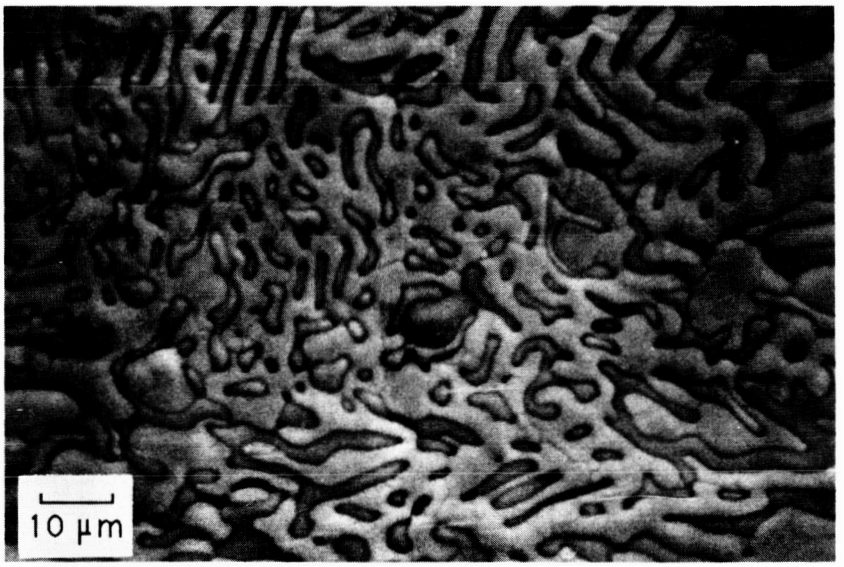

FIGURE 28. - ANOMALOUS EUTECTIC STRUCTURE FROM SURFACE OF A GROUND-BASED EUTECTIC SAMPLE WITH 31 K INITIAL UNDERCOOLING.

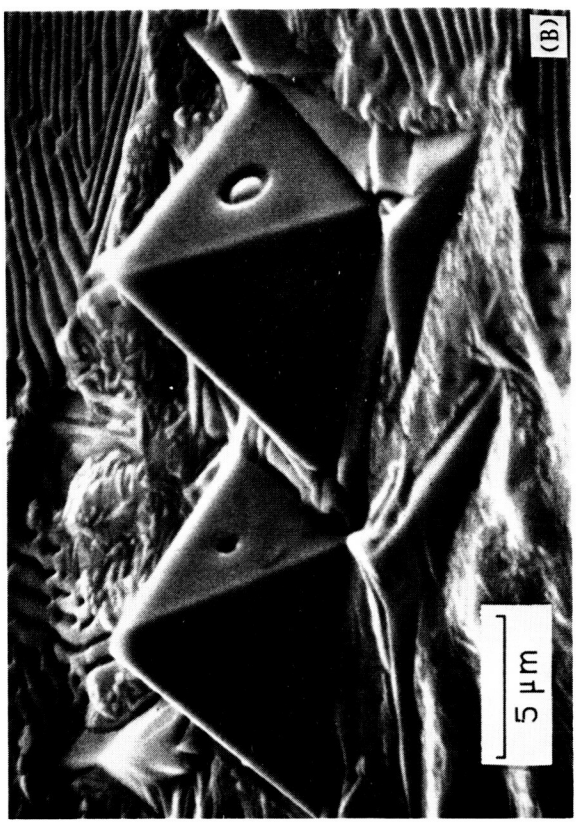

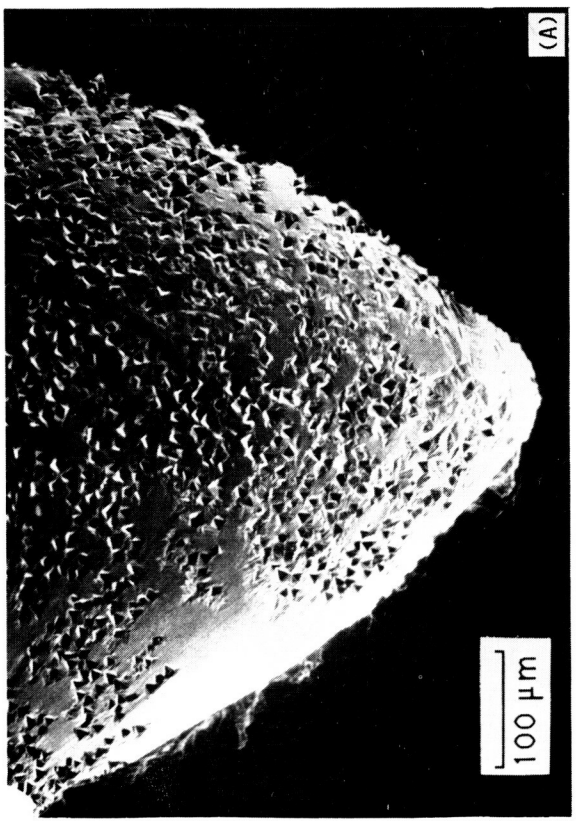

FIGURE 29. - FACETED CRYSTALS AT THE BOTTOM OF THE SHRINKAGE CAVITY.

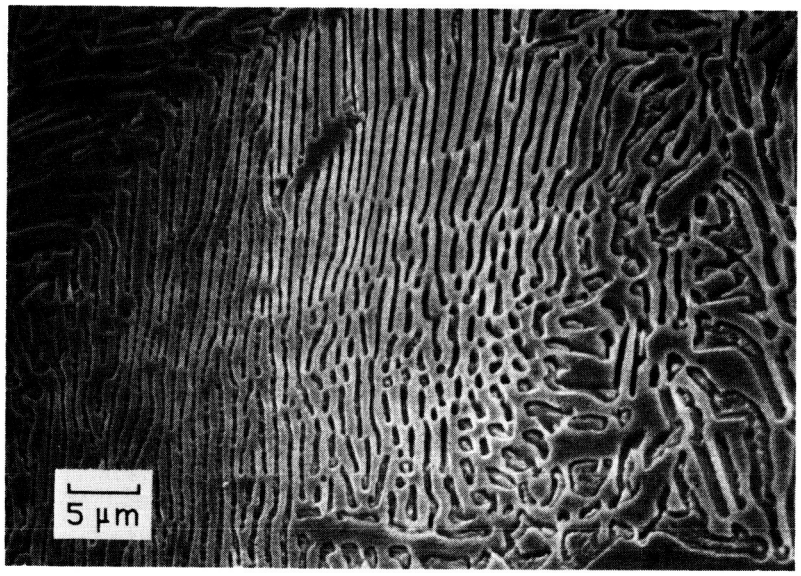

FIGURE 30. - CROSS-SECTIONAL MICROSTRUCTURE FROM THE FLIGHT SPECIMEN, SHOWING NORMAL LAMELLAR EUTECTIC.

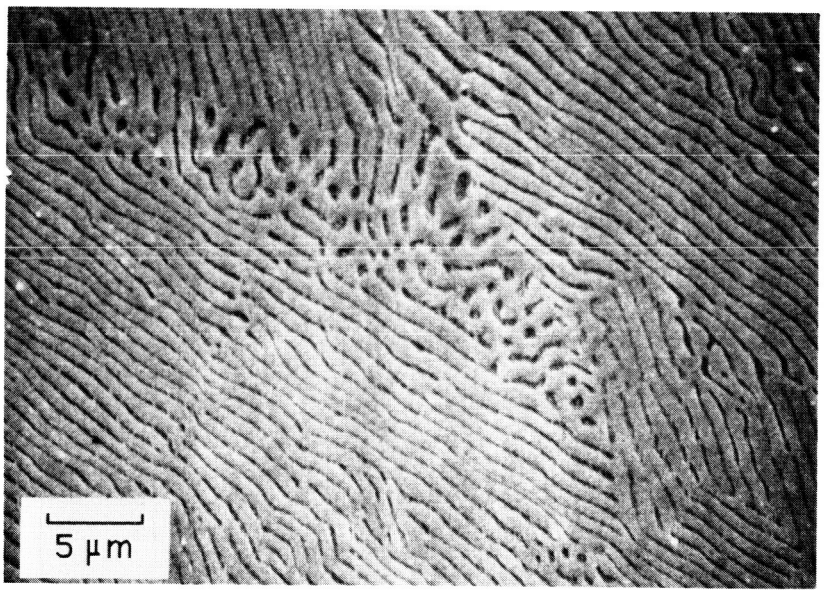

FIGURE 31. - CROSS-SECTIONAL MICROSTRUCTURE FROM A GROUND-BASED EUTECTIC SAMPLE WITH AN INITIAL UNDERCOOLING OF 31 K.

(B) TWO FACETED CRYSTALS AT HIGHER MAGNIFICATION.

(A) AREA WITH A DISPERSION OF FACETED CRYSTALS.

FIGURE 32. - CROSS-SECTION OF THE FLIGHT SPECIMEN.

1. Report No. NASA TM-88909 AIAA-87-0506	2. Government Accession No.	3. Recipient's Catalog No.

4. Title and Subtitle	5. Report Date
The Alloy Undercooling Experiment on the Columbia STS 61-C Space Shuttle Mission	6. Performing Organization Code 694-03-03

7. Author(s)	8. Performing Organization Report No.
Fredric H. Harf, Thomas J. Piccone, Yanzhong Wu, Merton C. Flemings, Yuh Shiohara, Lloyd B. Gardner, and Edward A. Winsa	E-3332 10. Work Unit No.

9. Performing Organization Name and Address	11. Contract or Grant No.
National Aeronautics and Space Administration Lewis Research Center Cleveland, Ohio 44135	13. Type of Report and Period Covered Technical Memorandum

12. Sponsoring Agency Name and Address	14. Sponsoring Agency Code
National Aeronautics and Space Administration Washington, D.C. 20546	

15. Supplementary Notes

Prepared for the 25th Aerospace Sciences Meeting, sponsored by the American Institute of Aeronautics and Astronautics, Reno, Nevada, January 12-15, 1987. Fredric H. Harf, NASA Lewis Research Center; Thomas J. Piccone, Yanzhong Wu, Merton C. Flemings, Yuh Shiohara, Massachusetts Institute of Technology, Cambridge, Massachusetts 02139; Lloyd B. Gardner, NASA George C. Marshall Space Flight Center, Marshall Space Flight Center, Alabama 35812; Edward A. Winsa, NASA Lewis Research Center.

16. Abstract

An Alloy Undercooling experiment was performed in an electromagnetic levitator during the Columbia STS 61-C mission in January 1986. One eutectic nickel-tin alloy specimen was partially processed before an equipment failure terminated the experiment. Examination of the specimen showed evidence of undercooling and some unusual microstructural features.

17. Key Words (Suggested by Author(s))	18. Distribution Statement
Binary systems (materials); Eutectic alloys; Nickel alloys; Solidification; Space Shuttle Mission 61-C; Electromagnetic levitator; Materials Science Laboratory; Levitation melting; Temperature measurement	Unclassified - unlimited STAR Category 26

19. Security Classif. (of this report)	20. Security Classif. (of this page)	21. No. of pages	22. Price*
Unclassified	Unclassified	37	A03

*For sale by the National Technical Information Service, Springfield, Virginia 22161